

# Launch Vehicle Selection and the Implementation of the Soil Moisture Active Passive Mission

Sarah Sherman  
 Jet Propulsion Laboratory  
 California Institute of  
 Technology  
 4800 Oak Grove Dr.  
 Pasadena, CA 91109  
 818-354-4791

Sarah.Sherman@jpl.nasa.gov

Peter Waydo  
 Jet Propulsion Laboratory  
 California Institute of  
 Technology  
 4800 Oak Grove Dr.  
 Pasadena, CA 91109  
 818-354-4796

Peter.J.Waydo@jpl.nasa.gov

Alexander Eremenko  
 Jet Propulsion Laboratory  
 California Institute of  
 Technology  
 4800 Oak Grove Dr.  
 Pasadena, CA 91109  
 818-354-4791

Alexander.E.Eremenko@  
 jpl.nasa.gov

**Abstract**— Soil Moisture Active Passive (SMAP) is a NASA-developed Earth science satellite currently mapping the soil moisture content and freeze/thaw state of Earth’s land mass from a 685km, near-polar, sun-synchronous orbit. It was launched on January 31, 2015 from Vandenberg AFB upon a Delta II 7320 launch vehicle. Due to external considerations, SMAP’s launch vehicle selection remained an open item until Project Critical Design Review (CDR). Thus, certain key aspects of the spacecraft design had to accommodate a diverse range of candidate launch vehicle environments, performance envelopes, interfaces and operational scenarios. Engineering challenges stemmed from two distinct scenarios: decisions that had to be made prior to launch vehicle selection to accommodate all possible outcomes, and post-selection changes constrained by schedule and the existing spacecraft configuration.

The effects of the timing of launch vehicle selection reached virtually every aspect of the Observatory’s design and development. Physical environments, mass allocations, material selections, propulsion system performance, dynamic response, launch phase and mission planning, overall size and configuration, and of course all interfaces to the launch vehicle were heavily dependent on this outcome.

This paper will discuss the resolution of these technical challenges.

## TABLE OF CONTENTS

1. INTRODUCTION .....	1
2. LAUNCH VEHICLE ASCENT TIMELINE.....	2
3. SPACECRAFT/LAUNCH VEHICLE INTERFACE .....	5
4. FAIRING ENVELOPE AND ACCESS .....	5
5. FUEL BUDGET .....	7
6. LV ENVIRONMENTS.....	7
7. LIFT CAPABILITY.....	8
8. CONCLUSION.....	8
REFERENCES.....	9
ACKNOWLEDGEMENTS.....	9
BIOGRAPHY .....	9

## 1. INTRODUCTION

The SMAP spacecraft provides a platform for the active radar and passive radiometer, which together measure global soil moisture and freeze/thaw at a high resolution and accuracy. These two instruments share the observatory’s most distinguishing feature, its deployable, boom-mounted, six-meter diameter parabolic reflector, which is part of an instrument assembly that spins independently from the spacecraft bus during science operations. Much of the Observatory’s overall configuration is driven by accommodation of this Reflector/Boom Assembly (RBA), either in its launch-stowed state, or in its on-orbit deployed, spinning state, shown in Figure 1.

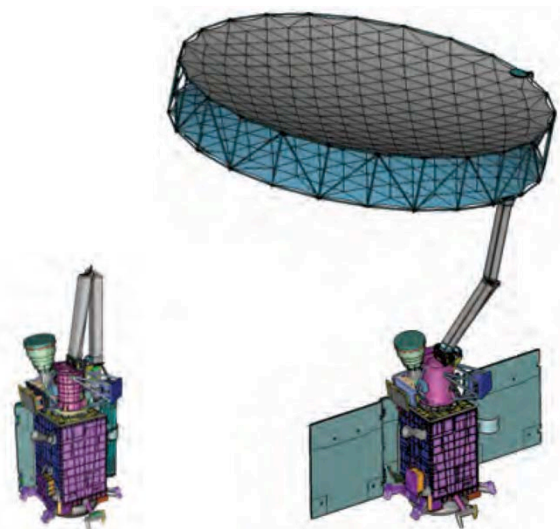
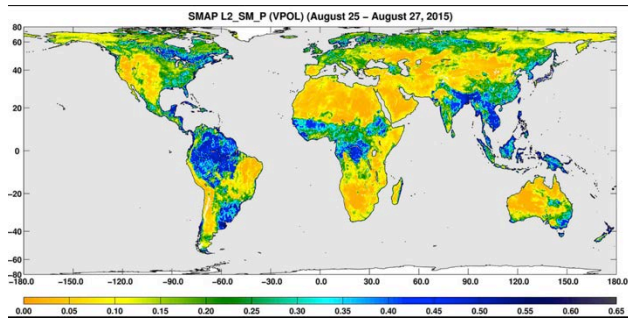


Figure 1. SMAP’s launch stowed (left) and on-orbit deployed (right) configurations [1].

The primary bus structure is comprised of four side panels, a top deck, mid deck, and bottom deck. All spacecraft and radar electronics are housed within the bus, and the radiometer and spin electronics are located on the

spun portion of the instrument structure. Attitude control is handled by a hydrazine propulsion system, an arrangement of four reaction wheels within the bus, and magnetic torque rods along each of the three primary axes. Coatings, blanketing, and exposed radiator area are used for passive thermal control.

Since its successful launch and commissioning, SMAP has been generating high accuracy and well-correlated soil moisture and freeze/thaw maps, as seen in Figure 2.



**Figure 2. Composite soil moisture data of the top 5 centimeters of soil for August 25-27, 2015. Dry areas appear yellow/orange, wet areas appear blue, and white areas indicate snow, ice or frozen ground [2].**

These results are contributing to our understanding of Earth’s water, carbon and energy cycles, climate and weather forecasting, as well as providing accurate flood and drought prediction.

NASA directed SMAP to maintain compatibility with multiple launch vehicles until the project’s Critical

Design Review (CDR) in July 2012 to accommodate the timetable needed for the launch service selection process. This presented an unusual set of design and implementation challenges, the resolution of which is detailed in the succeeding sections. Ultimately, the project successfully incorporated the chosen launch vehicle without impact to the launch date or the Observatory design, through a combination of appropriate design requirements and a flexible launch vehicle adapter design approach planned to incorporate this late selection.

## 2. LAUNCH VEHICLE ASCENT TIMELINE

The project was asked to evaluate the Minotaur IV+, Falcon 9, and Delta II launch vehicles. One of the major differences between these candidates and the chosen Delta II launch vehicle was the duration between liftoff and separation. SMAP was initially designed to support a 14-minute ascent before separating from the launch vehicle, autonomously counteracting tip-off rates using its hydrazine thrusters, deploying its solar arrays, and establishing 2-way communication with ground stations. SMAP’s pre-CDR thermal analyses, power analyses and operational concepts were developed according to this timeline. The selected Delta II’s ascent time was nearly 57 minutes for SMAP’s mass and injection orbit, resulting in the operations timeline shown in Figure 3.

Thermal and power analyses showed that this was unsupported by the existing spacecraft battery, so the expectations for launch phase events, including establishing communication, were changed.

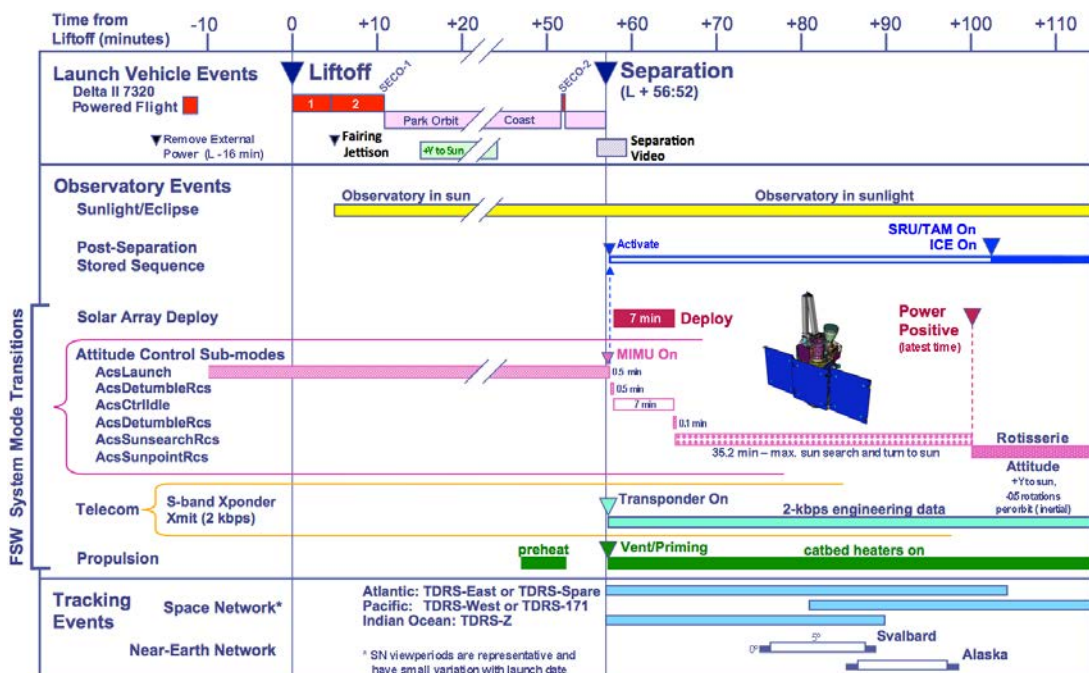


**Figure 3. SMAP launch timeline following liftoff.**

### *Catalyst Bed Heater Warmup Sequence*

The baseline launch behavior was designed to leave the eight attitude control thrusters' catalyst bed heaters off throughout launch vehicle ascent.

The catalyst beds had enough thermal inertia to stay above the undesirable "cold start" and damaging "frozen start" temperatures prior to their first use when reducing tipoff rates. Additionally, it avoided the risk of turning on the heaters in Earth's oxygen-rich atmosphere, which can cause permanent degradation or damage.

Upon updating the analysis for the Delta II ascent time of 56 minutes 52 seconds, it was shown that, for a conservative case, the catalyst beds could cool to 3.8°C by launch vehicle separation, which is considered a potentially damaging "frozen start," as shown in Table 1. It was necessary to run a pre-heat sequence during ascent to guarantee the catalyst beds reach a minimum temperature of 8°C at the time of the first detumble maneuver, while staying under 74°C in atmosphere. The solution would need to be tolerant to launch scrubs without subsequent ground intervention, and it must persist across an avionics reset. To protect against a stuck-on and stuck-off heater fault case, a combination approach was chosen: a fail-safe command sequence to turn on catalyst bed heaters for only 10 minutes during ascent, plus a flight software decision point at launch vehicle separation that extends the pre-heat duration in case any one catalyst bed heater temperature sensor measured less than 8°C. This strategy protects against credible single faults, including loss of a catalyst bed heater string and a Command and Data Handling (CDH) reset during ascent. It is noted that there is a two-fault case (CDH reset during ascent plus one catalyst bed heater string failure) that would have resulted in a thruster firing below 8°C, but still above the actual freezing point of hydrazine of 2°C.

**Table 1. Catalyst bed temperature effects**

<b>Temperature</b>	<b>Effect</b>
>74°C (air)	<b>Oxidation</b> - Oxidization of catalyst bed irreversibly damages thruster
>70°C (vacuum)	<b>Warm Start</b> - Nominal operation
8-70°C (vacuum)	<b>Cold Start</b> - Qualified for 1 planned, 8 unplanned
<8°C (vacuum)	<b>Frozen Start</b> - Potentially damaging

Since the catalyst bed heaters could not be powered on prior to liftoff due to oxidation concerns, the sequences

were running in the blind during ascent, an atypical practice for JPL. This resulted in the addition of a launch/hold criterion that the sequence kick-off must occur within a narrow time window, or else that day's launch attempt would be scrubbed.

### *Launch Vehicle Roll Attitude During Ascent*

Both the launch-stowed RBA and the Command and Data Handling (CDH) assembly were susceptible to overheating with the launch ascent's unique solar incidence angle. The longer ascent timeline mandated a launch vehicle longitudinal roll for the majority of the ascent to more evenly distribute solar radiative heating. This change was analyzed and accommodated by the launch vehicle provider, and necessitated several additional analyses by JPL.

### *Launch Vehicle Adapter Batteries*

Along with the lengthened ascent timeline came the need for increased battery capacity, as it would nominally be an additional 39 minutes and possibly as long as 97 minutes until the Observatory's solar arrays could be deployed and turned to sun. The 8S52P 78Ah Lithium-ion battery didn't have sufficient capacity to cover all margined ascent timelines. Due to the fact that its design, procurement, structural and thermal accommodations, and mass properties had already been established, it was necessary to augment the power storage system with additional batteries rather than simply increase the battery's size. The desire to minimally perturb the baseline configuration meant finding a suitable location for the additional batteries that would restrict hardware redesign to the least number of parts while minimizing impact to the overall architecture.

As the design of the Launch Vehicle Adapter (LVA), the main circular piece of primary structure between the bus and the launch vehicle, is tailored to the selected launch vehicle itself, it was the perfect candidate to house this new launch-vehicle specific hardware. A trade study examined several different battery chemistries, configurations, and usage strategies, their impacts to the power subsystem as a whole, as well as their compatibility with the thermal environment and physical accommodation. In addition, the close proximity to the launch vehicle separation hardware meant high levels of pyrotechnic shock may be encountered. Varieties of both primary (non-rechargeable) and secondary (rechargeable) batteries were considered. Ultimately, additional secondary Lithium-ion batteries were selected due to the available capacities, form factors, suitability for the environments, and compatibility with the existing power subsystem. To achieve the required capacity in the available volume within the LVA, three 8S10P 15Ah Lithium-ion batteries were added, increasing the Observatory's battery capacity by 45Ah or about 58%.

The battery's lowest predicted state of charge following launch vehicle ascent about 75%.

The cramped quarters and awkward physical access under the Observatory within the LVA presented challenging integration issues. A modular mounting system was devised allowing each of the three LVA batteries to be integrated or de-integrated individually without disturbing the others, as shown in Figures 4 and 5. Mounting structure and hardware was kept as common as possible between the three units, and part count was minimized and designs simplified to enable the compressed implementation schedule. Careful attention was paid to hand and tool access, lines of sight, and assembly flow to guard against slowdowns in the integration process. The necessity of exchanging test batteries for the flight units as late as possible in the integration flow, when schedule is most compressed, underscored the importance of practical, usability-based design and planning. The asymmetrical location of the group of LVA batteries aided in alignment of the Observatory's CG, reducing the need for dedicated balance mass.

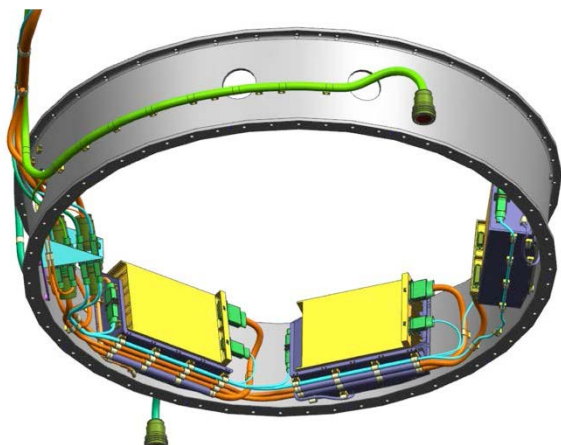


**Figure 4. LVA CAD model showing LVA battery subsystem details**

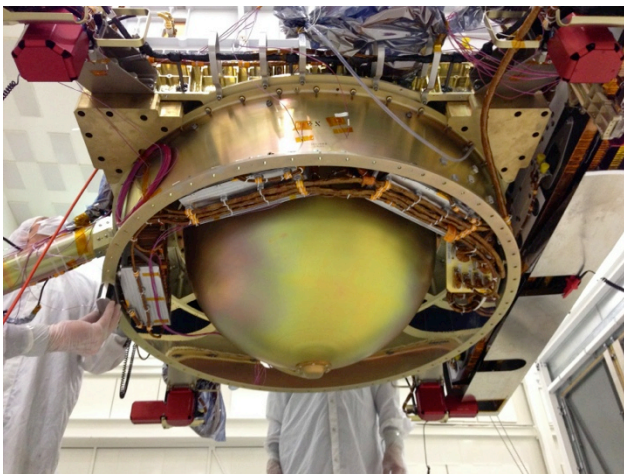


**Figure 5. LVA with additional batteries without MLI**

The decision had been made not to isolate the LVA batteries from the power bus after ascent, but rather to keep them online for the duration of the mission to provide additional margin during eclipses, out-of-plane maneuvers, and fault scenarios that might point the solar arrays off sun. Hence, there was a need to maintain a thermal environment conducive to long battery life. In the absence of LVA batteries, the baseline LVA was simple aluminum structure with Multi-Layer Insulation (MLI) blanketing on the exterior surface. Extensive thermal modeling showed that the new battery-laden LVA required both passive and active thermal hardware solutions to not only keep the LVA batteries in their operable range, but also to track the main battery temperature as closely as possible for the stability and long-term integrity of the battery system as a whole. Each LVA battery was mounted to a tray having thermostatically controlled heaters. The trays were isolated from the heat sink of the LVA structure with titanium standoffs, and each individual battery/tray assembly was wrapped in MLI. Lastly, the entire interior surface of the LVA was covered in Silver Teflon film to provide the appropriate emissivity value. Model results were correlated in system-level thermal-vacuum testing.

The new distributed nature of the Observatory's battery capacity led to some interesting harness design and usage considerations. Principally, the run from the LVA batteries to the battery arming plug, which was the confluence of all battery cables, was much longer than that of the main battery. Since the batteries all had to respond alike relative to the common power bus, the long LVA battery harness had to be impedance-matched to the shorter main battery harness. This was accomplished by tailoring both the number and gauge of individual conductors to the length of a particular run. Each LVA battery had its own power harness running to a cable bulkhead within the LVA. This bulkhead was placed at a 45° angle to provide easier mate/de-mate access and direct line of sight of the pins and featured keyed scoop-proof connectors to prevent mis-mating and shorting, as is standard JPL practice for power connections. Each 8S10P 15Ah LVA battery was internally balanced and brought to a precise state of charge before being mated to this bulkhead. Beyond the bulkhead, the three LVA battery harnesses merged into one, and were routed to a single connector at a field joint adjacent to the main battery connector, where they appeared as a single 8S30P 45Ah battery. The main 8S52P 78Ah battery was also internally balanced and brought to a matching state of charge before being mated at the same main field joint where the merged LVA batteries were mated. Immediately beyond this connection, all battery leads merged together at the battery arming plug, thereby appearing to the power bus as a single 8S82P 123Ah battery.

### 3. SPACECRAFT/LAUNCH VEHICLE INTERFACE

Most JPL spacecraft had the launch vehicle interface features machined directly into the primary structure adjacent to the separation plane. However, the Minotaur IV+, which was the presumptive launch vehicle for early SMAP design, features a third-party modular separation system, where the structure immediately on either side of the separation plane is supplied by a vendor and connects to the adjacent launch vehicle or spacecraft hardware via a bolted joint. Although this approach carries with it the scar mass of an additional major bolted joint in the primary structural load path, it allows the flexibility of decoupling the separation system and interface feature design from that of the rest of the system as a whole. The SMAP team's decision to carry this architecture forward regardless of the ultimate launch vehicle selection allowed design of the spacecraft structure to proceed in the meantime. Once the Delta II launch vehicle was selected, this separation interface structure, the Forward Separation Ring (FSR), was designed to bridge the gap between the launch vehicle separation plane and the aforementioned bolted joint at the aft end of the spacecraft in a structurally efficient manner, as shown in Figure 6. The FSR structure also carried the mounting brackets for the In-Flight Disconnect (IFD) cables (commonly known as umbilicals) and the separation connector for the SMAP instrument's nitrogen gas (GN<sub>2</sub>) purge line, which were launch vehicle specific. This followed the approach of focusing launch vehicle accommodation-specific hardware development to the smallest number of components possible.

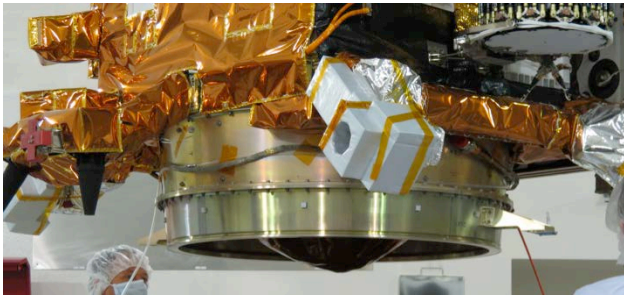


Figure 6. LVA bolted interface to FSR

#### Nitrogen Purge

The SMAP Observatory's spin mechanism required application of a constant GN<sub>2</sub> purge from early in the integration flow until liftoff. As this purge gas was supplied by the launch vehicle, it was necessary to incorporate a separation connector to safely decouple the GN<sub>2</sub> at the appropriate time in flight. Some candidate launch vehicles route this line to the payload via the fairing, and the fairing separation event provides the force to separate the purge line from the payload. Others route the purge line to a separation connector near the payload/launch vehicle separation plane, and the launch

vehicle separation event fulfills this function as well. SMAP's design up to its CDR had to accommodate either scenario. The Delta II employed the latter approach, and a standard purge gas separation fitting was incorporated into one of the IFD brackets on the FSR, directly adjacent to the separation plane.

#### Launch Vehicle Integration

Certain candidate launch vehicles, such as the Falcon 9, require horizontal integration of the payload to the launch vehicle rather than the more traditional vertical integration. This required that the SMAP structure be designed to have both the MGSE interfaces and structural load paths suitable for horizontal handling of the fully-integrated observatory. However, as the observatory would need to withstand transportation to the launch site in the horizontal position regardless, the horizontal integration wasn't a driving load case.

### 4. FAIRING ENVELOPE AND ACCESS

#### Envelope

The payload fairing envelope was the largest influence by far on the SMAP Observatory design, due to the need to accommodate all candidate launch vehicles. Out of all launch vehicle candidates, the Minotaur IV+ has the most restrictive usable volume, as shown in Figure 7, and this fact not only drove the overall size and external configuration of the Observatory, but also cascaded through nearly all aspects of the overall architecture. This presented end-to-end engineering challenges from the initial conceptual design all the way through the final System Integration & Test (SIT) operations.

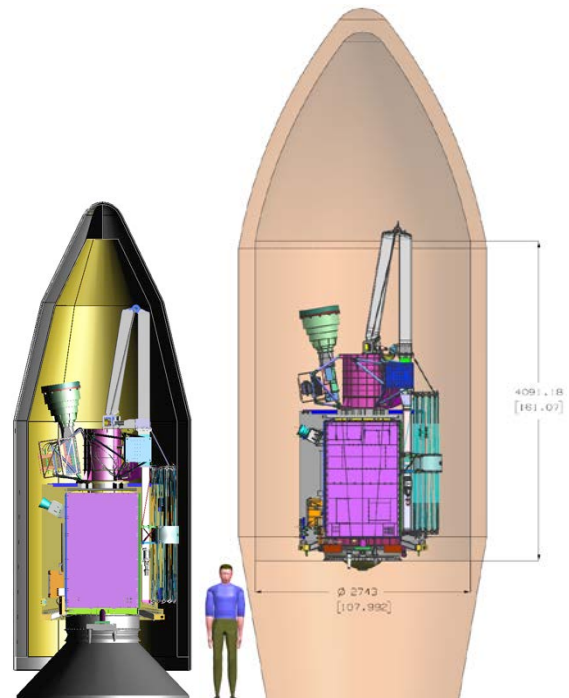


Figure 7. SMAP CAD model within Minotaur IV+

**(left) and Delta II (right) launch vehicle fairing envelope.**

Although SMAP's deployable reflector stows at a fraction of its final size for launch, the Minotaur IV+ fairing severely restricted placement options. Furthermore, the required deployed position and orientation of the reflector required the use of a multi-degree of freedom deployable boom, the configuration of which was complicated by the available stowed volume. Packaging this Reflector/Boom Assembly drove the overall bus structure dimensions, forcing all of the internal components into a confined space.

The chosen Delta II launch vehicle provided a much less restrictive payload fairing envelope. Although this alleviated many constraints, the selection came at a point that did not allow full exploitation of the relief, as the major architectural configuration had long since been established and component fabrication was already in progress.

One of the most challenging hardware accommodation efforts was for the Reaction Wheel Assemblies (RWAs). SMAP carries four relatively large RWAs, with three of them arranged in a rosette with its largest footprint in the horizontal plane. Proper arrangement of these three RWAs yielded a footprint slightly larger than the area available for their accommodation. As the size of the RWAs couldn't be reduced due to control requirements, mitigating design and procedural measures were implemented. These three RWAs had to be integrated into the bus structure as an assembly using complex, counter-balanced Mechanical Ground Support Equipment (MGSE) and an overhead crane in a time-consuming, manpower-intensive process, that involved a level of risk significantly higher than the individual integrations a larger bus structure would have enabled, shown in Figure 8. One of the adjacent side panels of the bus had to feature a clearance cutout, complicating load paths and therefore adding mass to the structure. This tight fit and complicated integration would have made unplanned removal for troubleshooting or rework risky and time consuming.



**Figure 8. Reaction wheel installation.**

These cramped quarters were similarly an issue for many of the Observatory's other internal components and subassemblies. Design compromises were required that forced an interdependent integration sequence, effectively burying certain components beneath layers of other components, secondary structure, and harness. The risks of this approach were realized when a deeply buried electronics box had to be removed for rework late in the integration flow, requiring execution of a convoluted removal and reinstallation procedure.

*Post-Encapsulation Access*

SMAP has two electrical interfaces that need to be accessed through the payload fairing door. The first allows direct access to the power bus for battery maintenance purposes and installation of the flight battery enable plug. The second interface allows various test configurations of the propulsion and pyrotechnic systems and installation of the flight arming plug.

In addition, the propulsion system has both gas and liquid service valves that require access through the fairing in the event of a contingency propellant offload situation.

It is desirable, and in some launch vehicle options, required, to have all of these points accessible through a single, relatively small fairing door. To that end, they were placed in close proximity to each other from an early stage. Selection of the Delta II meant one 24-inch diameter fairing door could be placed in a location of JPL's specification within an available range, which was broad enough to be compatible with the existing general layout. In the final Observatory configuration, the plugs and valves were moved into as close proximity as was practical, in a position and orientation tailored to the Delta II door. However, the relatively small spacecraft bus (driven by the Minotaur IV+ payload fairing envelope) coupled with the comparatively spacious Delta II fairing volume meant there was a significant reach from the fairing door to the plugs and valves. The electrical plugs

only needed to be accessed by a technician in standard clean room garb. The prop service valves, however, would need to be accessed by a technician in a bulky Self Contained Atmospheric Protective Ensemble (SCAPE) suit, which affords much restricted freedom of movement. Although a contingency prop offload event is highly unlikely, there is a requirement to demonstrate that such access is possible and practical. To prove feasibility, a simple mockup was constructed of a correctly sized Delta II fairing door with representations of the prop service valves in the appropriate positions within. Access in multiple operator positions, representing various possible access platform locations, was first modeled and then demonstrated using an actual SCAPE suit, seen in Figure 9.



**Figure 9. Access through fairing access door.**

*Solar Array Shape*

An early solar array configuration trade study weighed the number of solar cells, the ease of assembly and test, total mass, deployed panel impact to instrument and radio fields of view, and compatibility with the launch vehicle payload fairing volume. The ultimate result was a three panel “tri-fold wallet” deployable design, which stowed within the required volume, but featured no outward facing cells. However, the design’s two parallel hinges allowed for deployment testing in a 1g environment. Additionally, its construction and implementation was more straightforward than the alternatives, which included a design with five panels deployed on four hinge lines, and one with cells on the back of the outward-facing panel. The outward facing cells would provide power while the panels were still stowed during launch ascent, in a tumbling spacecraft scenario, or in a fault

scenario where the panels did not deploy correctly. This was seen as a good risk mitigation option, but since the total power provided by those outward facing cells could not support the spacecraft’s entire power draw, it was seen as a low-benefit option. Additionally, the Minotaur IV+ fairing volume constraints prohibited the increase in panel thickness that would arise from placing another layer of cells on the outward facing solar panel. The only way to accommodate these would be to reduce the total deployed panel area, which was not seen as a desirable trade.

**5. FUEL BUDGET**

The propellant tank is sized to accommodate fuel for attitude control, station-keeping, collision avoidance, correcting launch vehicle injection error, and a decommissioning de-orbit burn, with margin. With the Minotaur IV+ baseline, a  $\pm 18.5$  km perigee altitude injection error and the  $\pm 0.5$  %/sec per axis tip-off rates drove the use of an 80 kg capacity fuel tank. By comparison, the Delta II vehicle has  $\pm 9.3$  km perigee altitude injection error and  $< 1$  %/sec per axis tip-off rates [3, 5]. The ultimate selection of this launch vehicle caused a 14 kg reduction in the fuel requirement. At that point in the design, the benefits of implementing a smaller fuel tank were outweighed by the ramifications of a late-stage modification. The extra fuel capacity was seen as a beneficial margin against future orbit changes as well as a way to increase the mission lifetime via more allowable station-keeping maneuvers.

**6. LV ENVIRONMENTS**

As schedule required most key and driving structural design decisions be made prior to launch vehicle selection, a comprehensive dynamic environments envelope was established that bounded worst-case load cases from each of the candidate launch vehicles.

As shown in Table 2, the Falcon 9 has a relatively benign dynamic environment and was not the driving case for any of the launch loads as advertised, however the launch vehicle was still in its operational infancy and thus there was little abundant flight correlation for model-based loads, increasing uncertainty.

**Table 2. Summary of dynamic loads [3,4,5]**

	SMAP Envelope	Minotaur IV+ User's Guide 2006	Delta 2 7320-10C Payload Planner's Guide 2007	Falcon 9 User's Guide 2009
Axial Frequency	> 35 Hz	> 35 Hz	> 35 Hz	> 25 Hz
Lateral Frequency	> 15 Hz	> 15 Hz	> 12 Hz	> 10 Hz
Space Vehicle (SV) CG Limit Load				
Axial	+10.6/-2.0 G's	+9.5/-0.03 G's	+8.3/-0.2 G's	+6/-2 G's
Lateral	+/- 3.7 G's	+/-2.89 G's	+/-3.5 G's	+/-3.5 G's
Acoustic Env (Qual/PF)	144.2 dB	139.2 dB	142.7 dB	142.6 dB
Sep Shock Environment	4100 G's	2000 G's RUAG 937S	4100 G's for 3715 PAF	3000 G's
SV CG location (lateral)	< 1"	< 1"	< 2"	< 5"

The Minotaur IV+ provided the driving requirements related to lateral frequency and axial acceleration loads, the latter due to its all-solid propellant configuration, which accompanied the fact that it featured the shortest ascent timeline of the candidates. It also contributed the tightest requirement on the Observatory's lateral center of gravity, which SMAP controlled mainly via physical configuration and tuned with additional dedicated balance mass.

The Delta II was the source of the balance of the driving load cases, including the acoustic environment. Notably, its predicted separation shock levels are significantly higher than the other options, a factor that would ripple into the design of the LVA battery subsystem described above. Later, loads associated with the Main Engine Cut Off (MECO) event would require additional analysis to demonstrate margins.

This scenario yielded a final design that had positive structural margin against all load cases encountered on the selected Delta II, with ample margin against many, as shown in Table 2. However, although certain aspects of the Observatory appear to be overdesigned with respect to strength, the overall design is driven by stiffness, and margins are appropriate as such.

## 7. LIFT CAPABILITY

Launch vehicle lift capability drives a spacecraft's size, mass, redundancy, and complexity. SMAP was initially designed for the Minotaur IV+ not-to-exceed lift capability of 1156 kg. Low mass margin prior to Preliminary Design Review (PDR) drove the project to conduct an exhaustive mass reduction exercise. Some redundant units were eliminated from the baseline to bring the current best mass estimate in line with JPL's guidelines on mass margin throughout lifecycle development. Upon selection of the Delta II, the project stance was to keep the spacecraft designed to the same constraints to limit undue design ripples and cost. Mass increases due to launch vehicle selection, such as the LVA battery subsystem and the LVA/FSR bolted joint

scar mass, were inconsequential relative to the new capability. The resultant mass margin for the Delta II was high enough that it allowed for three secondary P-Pod CubeSat payloads to accompany SMAP, and it also allowed the project to solve late-breaking problems with mass. The observatory mass margin was tracked throughout the project lifecycle, as shown in Figure 10.

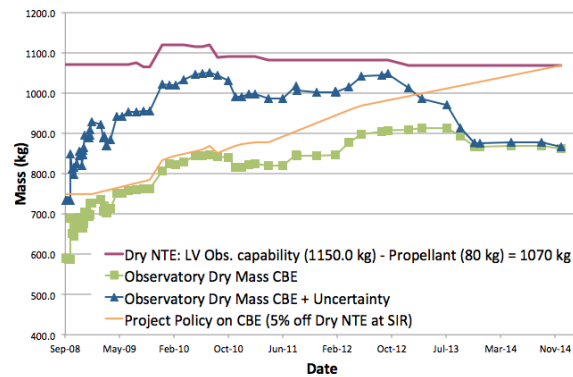


**Figure 10. Observatory mass estimate (green) stayed well below the launch vehicle not-to-exceed value (red) throughout the project lifecycle.**

## 8. CONCLUSION

Although SMAP's final form closely resembles the CDR-level design, several factors related to launch vehicle configuration and performance caused notable changes to ripple throughout the system. These impacted not just the design, but also the operation and performance of the Observatory.

Most aspects of the Observatory were designed to be agnostic to launch vehicle selection through the application of strategically chosen bounding restrictions. Other key components were left unfinalized until after selection so that they may accommodate launch vehicle specific hardware and interfaces. Limiting hardware changes to these areas allowed the rest of the design to move forward, maintaining the project schedule. Launch operational scenarios and command sequences were revised as dictated by launch vehicle performance.

As a result of this strategic approach, no effects of the timing of launch vehicle selection became critical-path items on SMAP's development schedule.

## REFERENCES

- [1] SMAP Handbook  
[http://smap.jpl.nasa.gov/system/internal\\_resources/details/original/178\\_SMAP\\_Handbook\\_FINAL\\_1\\_JULY\\_2014\\_Web.pdf](http://smap.jpl.nasa.gov/system/internal_resources/details/original/178_SMAP_Handbook_FINAL_1_JULY_2014_Web.pdf)
- [2] NASA JPL Earth Images:  
<http://www.jpl.nasa.gov/spaceimages/details.php?id=pia19877>
- [3] Minotaur IV+ User's guide (2013)  
<http://www.manualsdir.com/manuals/569830/orbital-minotaur-vi-minotaur-v-minotaur-iv.html>
- [4] Falcon 9 Guide  
<https://www.spaceflightnow.com/falcon9/001/f9guide.pdf>
- [5] Delta II Payload Planners Guide  
<http://www.ulalaunch.com/uploads/docs/DeltaIIPayloadPlannersGuide2007.pdf>

## ACKNOWLEDGEMENTS

Special thanks to the work and support of KSC's launch services program and ULA. The work described in this paper was performed by the Jet Propulsion Laboratory, California Institute of Technology, under contract with the National Aeronautics and Space Administration.

## BIOGRAPHY



**Sarah Sherman** received her B.S. in Mechanical Engineering and Aerospace Engineering from Princeton University in 2008 and her M.S. in Astronautical Engineering from University of Southern California in 2013. She has been with NASA's Jet Propulsion Laboratory since 2008, working as a Systems

Engineer on SMAP from early development through on-orbit operations. She is currently supporting the Mars2020 mission as a Mechanical Engineer.



**Peter Waydo** received a B.S. in Mechanical Engineering from Northern Arizona University in 2001. He worked on the mobility subsystem of JPL's 2003 Mars Exploration Rovers before joining the mission's System Integration and Test (SIT) team through both launches. After a subsequent stint in the automotive industry, he

rejoined JPL in 2011, eventually becoming the Mechanical Systems engineer for the later phases of the SMAP project. He then led the SMAP SIT Mechanical Team through launch. He currently serves as the

supervisor of the Mechanisms and Mobility Group within JPL Spacecraft Mechanical Engineering.



**Alexander Eremenko** received his master's degree in Aerospace Engineering from the Moscow Aviation Institute, Moscow, USSR (Russia) in 1984. He previously worked for Lavochkin Science & Production Association, Moscow, Russia for 11 years developing a variety of the planetary and astrophysical missions. For the

last 17 years Alexander has been working at NASA's Jet Propulsion Laboratory developing a variety of deep space missions including Aquarius, Mars Exploration Rover, Mars Science Laboratory, SMAP, supported multiple proposals and technologies development. He is currently the Product Delivery Manager for the Mechanical subsystem of the Europa Multiple-Flyby Mission.